

Expanding the sensory and perception horizon of an autonomous robot through the communication system

¹Mr. Haydar Sabeeh Kalash, ²Dr Renu Kachhoria, ³Dr. Anandakumar Haldorai, ⁴Ms. Maria Talib Al Amri, ⁵Dr. Ram Subbiah, ⁶Bharathababu K

*1 Lecturer in Faculty of Computing Sciences, Gulf College Muscat - Sultanate of Oman
haydarsk@gulfcollege.edu.om*

2 Assistant Professor, computer department, Pimpri Chinchwad college of Engineering, Pune. renu.iita@gmail.com

3 Professor (Associate), Department of Computer science and engineering, Sri Eshwar College of Engineering, Coimbatore, Tamil Nadu, India, 641202. anandakumar.psgtech@gmail.com

4 Lecturer in Faculty of Computing Sciences & Head of Industry and Community relations department, Gulf College, Muscat - Sultanate of Oman. Marya@gulfcollege.edu.om

5 Associate Professor, Mechanical engineering, Gokaraju Rangaraju institute of Engineering and Technology, Hyderabad. ram4msrm@gmail.com

6 Assistant Professor, Anand Institute of Higher Technology, Chennai-603103. kbharathababu@gmail.com

ABSTRACT

Purpose of the research: Among the most pressing concerns in the domain of public robotics is giving robots the capacity to focus their concentration on the person with who they engage. Different systems combine oral and visual signals to locate a person utilizing several sensors, utilizing bio-inspired principles. However, because many of the fusion techniques are developed for stationary systems, like the one used in video-conference centres, they might encounter issues when applied to the sensory devices of the robot. Inside the scenario of the volume, robotic understanding states the machine learning methodologies which allows machine to understand from sensorial information depending on learned models, respond, and act.

Recent Findings: The previous advances that took place in ML, particularly deep-learning techniques, robotic insight methods have been changed in a manner where latest strategies and activities have become a actuality.

Summary: Latest events in human being-robot communication, complicated mechanical activities, intellectual understanding, and option-building, in part, the outcome of ML algorithms are well-known progress and success. This study will analyse the strategies for developing intelligent perception systems in robots and address current and future themes and use-cases.

Result: The studies indicate that the planned technique for a proactive speaker discovery and tracing in a human-robot collaborative framework has promise.

Keywords: multi-modal perception, robotic perception, artificial intelligence, machine learning.

1. Introduction

The most common use for robotics is to support factors in their daily routines. Indeed, throughout the last 2 centuries, there's a concerted push to investigate and construct what is commonly referred to as service robots. Psychotherapy, recuperation, teaching, and simply serving as a recreational companion are some examples. Many of the major findings from advanced human-computer

intercommunication research is generalized to person-robot interactivity. According to [1], the recent fusion of humanism and constructing techniques for the improvement of the life of a human, springboard for breakthroughs intwenty-first centurial. Embodied cognition are related to the premise that a machine can learn knowledge structures through interaction with and exploring the outside environment physically.

Cognitive robots are presently outfitted with many sensors to achieve this goal and are powerful. The huge amount of data given by various types of sensors should be analysed and handled in a fast adequate time to allow proper interaction between robots and people [2]. The selective attention and Multi-modal perceptioncombine to be techniques for dealing with these challenges [3] and guiding and constraining social engagement [4]. Services or social robots can target their concentration on humans before responding to human activities, according to the perception and the quality of the work. This paper assesses the advantages of combining auditory and visual data in a sustained concerned frame to track a single speaker in an out-of-control and interactive environment.The robotic Perception system is shown in Figure 1.

The utilization of many sensory modalities improves the wholeness of the robot's perception and representation of its environment. Several types of sensors give broad limitations to be undermined, and its integration usually enhances the quality achieved by adding separate sensors. The main technique for embedding audio data into a robot's perceptual function is to monitor a speaker. Most of the computing auditory scene investigation and sound origins localization techniques utilized in voice communicating applications (YouTube clip, speaker classification, voice identifier) have been lately included in the tracking reasons of robotic area ([5,6]). They're based primarily on spectral analysis and the time difference of arrival (TDOA).

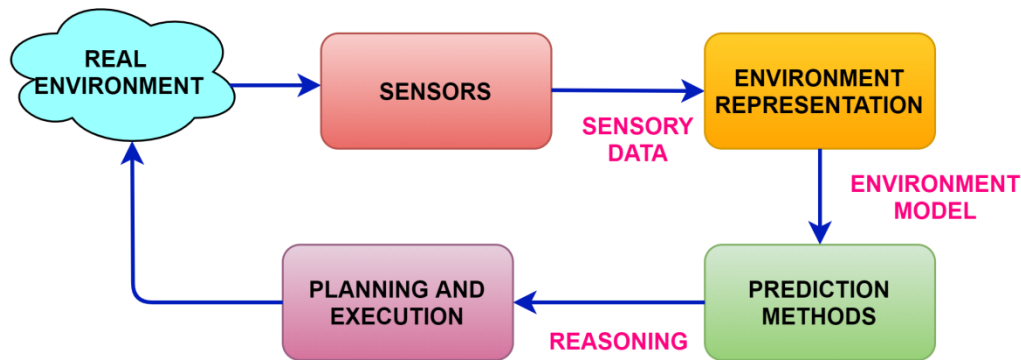


Figure 1: Robotic perception system.

Robotic perception,which includes everything from self-organizing grid maps to object detection, is critical on machine to draw conclusions, method, and function in actual surroundings. Hurdle discovery [7, 8], object identification [9, 10], semantic site categorisation [11, 12], 3D environment identification [13, 14], expression and audio recognition [15], events classification [16], terrain categorizing [17], road identification [18], pedestrian discovery [19], activity recognition, are the examples of robotic perception subareas that include self-determining robot-vehicles. Machine learning methods, varying against traditional on deep-learning strategies, are now used in many robotic

vision systems [20]. Unrestricted learning, controlled classifiers employing hand-crafted features, deep-learning neural model examples are convolutional neural network, or maybe a mixed-method approach can be also used for robotic vision.

Information given by sensor(s) is a crucial ingredient of robotic vision, irrespective of the proposed method used. Information can originate from one or more sensors seated onboard the robot, and it can originate from the architecture or some other robot (e.g., cameras seated on UAVs flying closely). An efficient solution is usually required to aggregate and analyse the input from the sensors, until an ML technique can be used in multiple-sensor vision, whether the clone modality or multimodal. Based on the severity of the issue and the kinds of sensors utilized, data arrangement and correction steps are required. Sensor-related environment recognition is a crucial piece of mechanical network. Mapping typically refers to the pair of adoption of a metric system as well as associated to semantic translation and is thus synonymous with atmosphere identification.

Mapping is a synod for ecosystem depiction since it includes both the pair of possession which includes measurement system and semantic translation. The semantic mapping adopts machine learning at several levels including thinking on volumetric occupation and ecstasy, as well as recognizing, describing, and ideally fitting local areas from diverse duration, i.e. not just higher-level explanations. The most important function of environment mapping in many of these cases is to describe information from exteroceptive sensors on-boarded on the robot designed to facilitate thinking and inferences about the real-world situation in which the robot works. Perception functions of robots, such as positioning and movement, are influenced by the environment in which they work. In essence, the robot is constructed to work in one of the two environments: inside or outside.

As a result, alternative assumptions might include in the mapping (depiction) and perception systems for both interior and outside situations. Furthermore, the sensors employed vary based on nature, so the sensory input that needs to be handled by a perception system for interior and outdoor settings will indeed be varied.

Many indoor robots presume that the surface is frequent and plain, which helps with environment representation models in certain ways; on either side, for the outside field the robot's terrain is frequently irregular, making environment modelling an obstacle by itself, and without a fair treatment, consequent perception activities are negatively impacted. Furthermore, robotic perception outside must contend with changing climatic conditions as well as fluctuations in lighting conditions and spectrum.

2. Contribution

Contributions of the work are given below:

- 1) Increasing the visual system's reliability by using a probability description of people's positions. Video evidence is defined by the explanation formed by the histogram.
- 2) For a range of situations, evaluating the efficiency of the visual localization network only accompanied by OpenCV features-sensor (alteration in illumination, make a mess up, and blockage). Face-detectors, namely those included in the OpenCV package, frequently employed in the robotics industry for tracking reasons.

- 3) In the real world, a communicative speaker is used for examining the auditory perception technique using binaural cues. The auditory system is built using two microphones and the Generalized Cross-Correlation framework (GCC) and the other one is PHAT (phase transform) approach to compute the density function of the degrees of arrivals.
- 4) Developing a strategic method for combining visual and aural inputs in the creation of a multimodal sensor. Bayesian inference framework is based on the fusion method.

3. Literature Review

The occupancy grid mapping [21] method is the most prominent alternative inherited from surrounding depiction for transportable automation and independent robotic machine. Because of its effectiveness, probabilistic foundation, and quick execution, such 2-Dimension charting is utilized in multiple transportable systems. Even though many techniques employ 2-Dimension-construct illustrates to depict the actual globe, 2.5-Dimension, and 3-Dimension description system have become popular. There are two main motivations for adopting high dimension representations:

- (1) In more complicated situations, when 2D depictions are inadequate, robots are required to travel and make judgments.
- (2) Because contemporary 3D technological solutions are cheap and dependent, 3D environment depicts the now possible. The latest advancements in application software such as Robot Operating System and Point Cloud Library, as well as the introduction of techniques such as Hornung et al. Octomaps's [22], have all contributed in rise of three-dimensional-atmosphere depictions.

The introduction, widespread use of RGB-D depth in sensors allowed for creation of bigger and highly accurate 3-Dimension charts. A lot of work has gone into semantically identifying these mappings at the pixels and voxel levels. The most applicable approaches may be divided into two categories: online-only methods and offline-only methods. Online approaches analyses information obtained using transportable robot and progressively create a semiotics chart. Such approaches can be frequently used in conjunction with a SLAM framework, which maintains the map's geometrical integrity. Creating maps for the atmosphere is a vital element of every mechanical model, and it's also well-studied. A piece of sequential localization and mapping (SLAM) issue, early work combined mapping and localization [23, 24]. Work has concentrated with or embedding period (brief or extended word) into the internal mechanism and utilizing the matrix chart stated in [25], pose-graph depictions as stated in [26], and distribution curve transform (NDT) as reported in [27].

RGBD data is evaluated using a spontaneous forest-based decoder to anticipate semantic labels, as reported by Hermans et al. [28]. These labels are regularised using the conditional random field (CRF) approach suggested by Krahenbuhl and Koltun [29]. Likewise, McCormac et al. [30] fuse CNN forecasts relate to the environment inside a mathematically coherent chart using the elasticity fusing SLAM technique described by Whelan et al. [31]. The CNN is utilized to progressively create an interpretation chart in the study of Sünderhauf et al. to increase the total category covered by CNN and augmenting it with a sequence of yet another filter that could be taught on-line. Variety of semantic chart methods developed to work off-line, using a thorough chart world as input. Large-scale signals of

interior structures are handled in the categories listed by Ambrus et al. [32, 33] and Armeni et al. [34], and then, after that, after segmenting the data given as a piece of information, the result is in “rooms.”

Armeni et al. work with multi-floor systems by tracking the areas between both the barricades, ceilings, and other surfaces, accompanied by the restriction, constructed wall must exist in axis symmetrical. Ambrus et al. utilize 2Dimensional cell-complicated graph-cut method to validate the differentiation with the major barrier that unique one-story constructions could be handled (i.e., the Manhattan world presupposition). We can expand this research by using the Bayesian model to combine multiple forms of data (phonic and view) and combine both the top-down and bottom-up data visually, all within the context of the Bayesian coding hypothesis [35]. Nakadai et al. [36] presented the first experiment measuring the real-time audio and viewable. They represented a simulation-based evaluation of past comparable initiatives and noted that auditory analysis and combined perception are now dependent on immature technologies and lacked real-time analysis. To drive the focus cohesion, they devised a strategy based on the formation of aural, visual, and related streams. A top-down design focused on utilizing the suggested approaches of the combined feature and voice recognition was emphasized as a potential solution to counter alterations in the surrounding circumstances (illumination, resonance, background noise), yet at the expense of actual-time computing.

Bayesian model have been regarded as an effective technique for data fusion. Asano et al. [37] used this technique to model the combined probability distribution of voice / visual sensors to estimate their engagement co-occurrence, which had been linked with the identification of a speaker. Back-ground subtractions were used for visual tracking, while the MUSIC technique was used for aural tracking. They developed this technique as part of strong speech classifiers that could tolerate environmental disruptions. As a consequence, testing was carried out in a controlled environment with a 60-degree ring around the monitoring apparatus and a constant speaker configuration. They also described an off experiment [38], wherein they utilized a model-based strategy to adapt their technique in response to a periodically changing environment. They used the gadget placed on the humanoid HRP-2 to follow single wandering individual in a confined environment.

4. VISUAL AND AUDIO TRACKING SYSTEMS

4.1. Acoustic Direction of Arrival (DoA) evaluation

The installation of an auditory monitoring system necessitates the use of a method that enables one to predict the signal's position and orientation (DoA). The PHAT (phase transform) method, which is part of the generalized cross-correlation (GCC) architecture, is used to accomplish the acoustic DoA estimation in our approach. The PHAT technique is recognized as GCC technique which is a notably stable technique for no stationary noise and reverberated via trials in actual settings. Clustering approaches are identified as a viable solution for multi-source identification.

Figure 2 depicts, the widespread cross-sectional, $\varphi_{x_1x_2}^g(\tau)$ is represented using the cross power spectral density function, $\Phi_{x_1x_2}(f)$ shown in (1):

$$\varphi_{x_1x_2}^g(\tau) = \int_{-\infty}^{\infty} \psi_g(f) \Phi_{x_1x_2}(f) e^{j2\pi f\tau} df \quad (1)$$

x_1 and x_2 are the signals caught on the 2 microphones, $\psi_g(f)$ is a weighting function where PHAT weighting is determined as:

$$\psi_g(f) = \frac{1}{|\Phi_{x_1x_2}(f)|} \tag{2}$$

The cross-power spectral-density activity, generated within every aperture employing thousand twenty-four examples Fourier transforms by Fast Fourier Transform and hybrid-checking is generated using the opposite Fourier transform via IFFT, as shown in Figure 2. The great height in the corresponding purpose is researched accompanied by a greater resolve using a parabolic interpolation step. The TDOA ($\hat{\tau}$) is calculated for every analysis window, and the associated angle is given as:

$$\hat{\theta} = across\left(\frac{c\hat{\tau}}{d}\right); \text{ being } \hat{\tau} = \underset{\tau}{\operatorname{argmax}} \varphi_{X_1X_2}^g(\tau) \tag{3}$$

Here $c=343$ m/s (approximate temperature for laboratory 20°Celsius) the fastness of the sound, d is the dissolution uniting mics (13.5 centimeter).

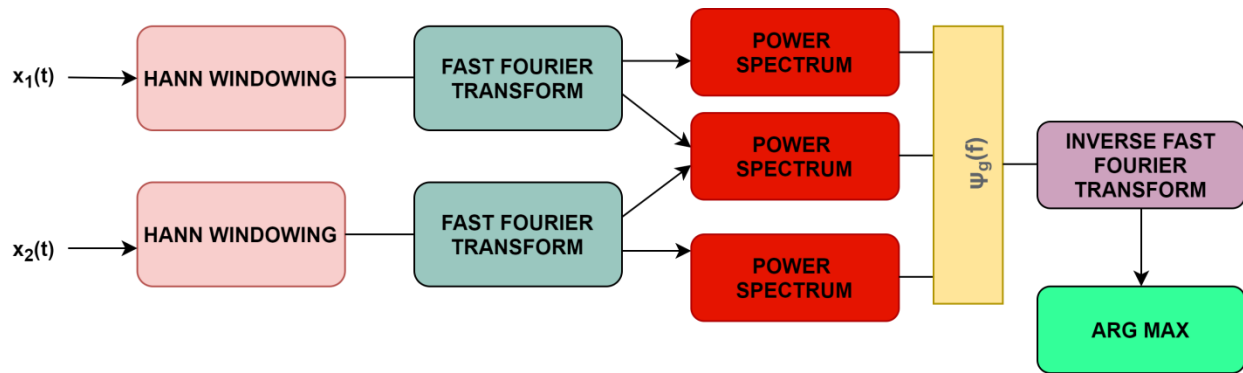


Figure 2: Phase transform block diagram

4.2. Proto-Objects Localization Histograms

The segmentation module displays list of proto-objects together accompanied by their corresponding picture locations and saliency. Those proto-objects are rearranged derived from location (axis transition) represented in horizontal and vertical gradients corresponding to the original robotic posture, taking into account the camera model. A histogram is created located on the azimuth gradients of the proto-objects based on the noticeable rate per every ten segmented pictures (about 1 s). Proto-objects positioned in gradients accompanied by higher saliency is specified by extra heaviness in accumulation procedure to achieve a more precise and steady assessment of the person's position. Furthermore, the mean saliency rating (scale from 0 to 255) of the nearby environment is calculated and set as a saliency threshold within the first instant of recording. Proto-objects having a saliency underneath this level are ignored and then histogram aggregation is not generated.

The video proof is a histogram that indicates the likelihood of finding a human in each location. It depicts the probability's function estimates the actual evidence of a human situated within 0 and 180 degrees surrounding a mechanical head, using an equi-width histogram of 10 bins. The vector is represented as a histogram rate $p(V) = [p(V_{0-10}), p(V_{10-20}), \dots, p(V_{170-180})]^t$ which denotes

chances of possessing a human within the specified span. To make it simpler, the specified span is denoted ranges are as Θ_i with $i = 1..18$, here the i -th span denotes the localization within gradient $(i - 1) \cdot 10^\circ$ and $(i) \cdot 10^\circ$. Consequently, the viewable histogram is denoted as $p(V) = [p(V_{\theta_1}), p(V_{\theta_2}), \dots, p(V_{\theta_{18}})]^t$. For example, the data denotes a greater chance of possessing a human in the case, Θ_{10} , which is given as in the specified span of $100^\circ - 110^\circ$.

4.3. Acoustic DoA Histograms

A probabilistic approach using a histogram structure is used to create a reliable assessment of the DOA angles' audio. This histogram was created by averaging the DoA angles. The intensity of peripheral noise is calculated for 1 s at the start of the trials, to precisely choose the films with a particular amount of voice energy. As a result, estimates derived in casement between the ability to exert effort below the earlier defined limit were rejected derived from that starting ability to exert effort. The limit can be adjusted based on the surroundings in these tests, it's determined to be the amount of energy required to detect a low-pitched speaker at 4 meters. The vector is used to represent: $p(A) = [p(A_{0-10}), p(A_{10-20}), \dots, p(A_{170-180})]^t$.

It is depicted as: $p(A) = [p(A_{\theta_1}), p(A_{\theta_2}), \dots, p(A_{\theta_{18}})]^t$.

4.4. Fusion

The inferences built across a Bayesian network to integrate audio and visual information. This system is constructed to depict the combined probabilities of audio (calculated Do A gradient of probable sound origin) and visible circumstances (position of feasible proto-objects denotes a speechmaker or a clamorous human). The variable to assess relates to the chance of possessing a person that talks or produces noise from a certain variety of angles, depending on this joint possibility.

The network utilized and the potential values of the three factors evaluated. As observed, audio data are recorded by N_a sound nodes, which correlate to 18 different angle values or bins for auditory source discovery systems. Similarly, vision data is recorded by N_v nodes, which is linked to 18 monitoring angles varies where segmentation proto-objects relating to a person might be given. As a result, the 18 potential areas where visual and auditory sensors can also be engaged match N_s . This network's assumption is only used when sound is recorded. If the level of acoustic energy doesn't suggest that a person is there, the video data is used to route them.

In histograms, the probability situation of the variables investigated is represented by all the other vectors. These histograms alter concerning time whenever the sensor upgrades the aural and visual data by producing the sensor proof, $p(X)$, as shown in the picture.

$$p(X) = \left(\frac{p(A)}{p(V)} \right) \tag{4}$$

Bayes network provides with calculating, histogram connected with spokesman's location

$p(S) = [p(S_{\theta_1}), p(S_{\theta_2}), \dots, p(S_{\theta_3})]^t$ and the evolution of the azimuth gradient is achieved below:

$$\hat{\Theta} = \arg \max P \left(\frac{S}{X} \right) \cdot p(X) \tag{5}$$

4.5. Inference Process

The status provided by the output layer or the speakers calculated using a Bayesian network inference method, as discussed in the preceding section. As a result, the status of "S" may be established by calculating its chances of distribution ("posteriori" potential is probability distribution given after all relevant information is considered), which is linked to using the grid.

$$P(S/X) = (P(S/A)|P(S/V)) \tag{6}$$

The deductions of sound/video predictions are presumed to be almost independent once S is permanent to a specified state, even though at one point the impact of familiar source (the addresser positioned in a particular location observed the whole time using webcams) is taken away originating at the allocation, the autonomous clamorous variance of predictions rests. Namely, perfect sensors might only have one peak near 100 histograms. However, intrinsic noise (cohesive or inconsistent noise) and ambient acoustic characteristics (chronic pain, dispersion, etc.) impact the hearing sensor, which is separate from the intrinsic noise of the visual sensor.

A formula may be used to calculate the conditional probability or a posteriori probability depending on this assertion:

$$P\left(\frac{S}{X}\right) \cdot p(X) = P\left(\frac{X}{S}\right) \cdot p(S) \tag{7}$$

S is supposed to have a flat prior allocation (it represents a priori assumptions on the presenter location). Therefore, $P(S_i) = 1/Ns$.

After calculating the conditional probability, the histogram with respect to p(S) distribution function is constructed using Bayes theory in evidential chances (p(V) and p(A)) acquired every 1 s from the auditory and visual sensing. An equation may then be used to predict the location of the speaker or a loud individual (6).

4.6. Training Phase

The conditional probability table is also known as the likelihood table, is derived from teaching images and depicts why the sensor assessment is affected by the original value, environment data, and sensor activity. Throughout the training phase, the robot's neck is retained in its original posture. Audio and visual modules generated histograms for every step, which is utilized to construct each column of the conditional probability matrices below,

$$P(X/S) = (P(A/S)|P(V/S)) \tag{8}$$

$$P\left(\frac{A}{S}\right) = \begin{pmatrix} p(A_{\theta_1}/S_{\theta_1}) & p(A_{\theta_2}/S_{\theta_1}) & \cdots & p(A_{\theta_{18}}/S_{\theta_1}) \\ \vdots & \vdots & \ddots & \vdots \\ p(A_{\theta_1}/S_{\theta_{18}}) & p(A_{\theta_2}/S_{\theta_{18}}) & \cdots & p(A_{\theta_{18}}/S_{\theta_{18}}) \end{pmatrix} \tag{9}$$

And the audio histograms recorded for each speaker position are represented by the conditional probability matrix:

$$P\left(\frac{V}{S}\right) = \begin{pmatrix} p(V_{\Theta_1}/S_{\Theta_1}) & p(V_{\Theta_2}/S_{\Theta_1}) & \dots & p(V_{\Theta_{18}}/S_{\Theta_1}) \\ \vdots & \vdots & \ddots & \vdots \\ p(V_{\Theta_1}/S_{\Theta_{18}}) & p(V_{\Theta_2}/S_{\Theta_{18}}) & \dots & p(V_{\Theta_{18}}/S_{\Theta_{18}}) \end{pmatrix} \quad (10)$$

$P(X/S)$, the a posteriori matrix $P(S/X) = (P(S/A)|P(S/V))$ is computed as:

$$P\left(\frac{S}{A}\right) = \begin{pmatrix} \frac{p(A_{\Theta_1}/S_{\Theta_1})}{Z_1} & \frac{p(A_{\Theta_2}/S_{\Theta_1})}{Z_2} & \dots & \frac{p(A_{\Theta_{18}}/S_{\Theta_1})}{Z_{18}} \\ \frac{p(A_{\Theta_1}/S_{\Theta_2})}{Z_1} & \frac{p(A_{\Theta_2}/S_{\Theta_2})}{Z_2} & \dots & \frac{p(A_{\Theta_{18}}/S_{\Theta_2})}{Z_{18}} \\ \frac{p(A_{\Theta_1}/S_{\Theta_{18}})}{Z_1} & \frac{p(A_{\Theta_2}/S_{\Theta_{18}})}{Z_2} & \dots & \frac{p(A_{\Theta_{18}}/S_{\Theta_{18}})}{Z_{18}} \end{pmatrix} * 1/N \quad (11)$$

Where $N = N_a + N_v; Z_i = p(A_{\Theta_i}) = \frac{1}{N_s} * \sum_{k=1}^{N_s} p(A_{\Theta_i}/S_{\Theta_k})$ for $i=1..N_a$.

$$P\left(\frac{S}{V}\right) = \begin{pmatrix} \frac{p(V_{\Theta_1}/S_{\Theta_2})}{Y_1} & \frac{p(V_{\Theta_2}/S_{\Theta_1})}{Y_2} & \dots & \frac{p(V_{\Theta_{18}}/S_{\Theta_1})}{Y_{18}} \\ \frac{p(V_{\Theta_1}/S_{\Theta_2})}{Y_1} & \frac{p(V_{\Theta_2}/S_{\Theta_2})}{Y_2} & \dots & \frac{p(V_{\Theta_{18}}/S_{\Theta_2})}{Y_{18}} \\ \frac{p(V_{\Theta_1}/S_{\Theta_{18}})}{Y_1} & \frac{p(V_{\Theta_2}/S_{\Theta_{18}})}{Y_2} & \dots & \frac{p(V_{\Theta_{18}}/S_{\Theta_{18}})}{Y_{18}} \end{pmatrix} * 1/N \quad (12)$$

Where $N = N_a + N_v; Z_i = p(V_{\Theta_i}) = \frac{1}{N_s} * \sum_{k=1}^{N_s} p(V_{\Theta_i}/S_{\Theta_k})$ for $i=1..N_v$.

5. Experimental Analysis

Several circumstances of illumination, background, and environmental noise are used to evaluate the viewable and aural systems. The tests were carried out along with the robot's head in a stationary posture and a human wandering over it, standing in various poses and against backdrops (the head of the robot is displaced physically). The viewable and auditory histograms are used to make the measurements. Inclusion with that the photograph took using the camera present on the left side of the stereo-vision system is safeguarded in single-channel pictures. The identification achieved by testing the system is depicted using a red circle in such pictures. Blue circumferences are painted around the faces assessed by a facedetector. This data is used to demonstrate the potential merits and limits of various approaches when compared to the frequently utilized instrument for monitoring individuals. Two separate tests are being used to evaluate the multimodal sensor, which combines the results of the optical and aural systems. Configurations were conducted using two experiments: 1) The first study deals with stationary arrangements while a person talks near the head of a robot. 2) The next one deals with upgrading the position of the robot head concerning the inferred angles (the greater chances of having the person who talks to the robot), using a Head Robot Control Service.

The visible system was created with the primary goal of identifying speakers in mind. As a result, the system calculates the noticeable of proto-objects by providing the skin-color attribute the most

heaviness but also considering other traits that may be beneficial for activities that do not need the presence of a human. The system was evaluated by positioning the robot's head across from five distinct backdrops and under varied lighting circumstances to assess the durability of the histograms constructed on the proto-objects in an actual environment with diverse complex backgrounds (morning and dark time). Figure 3 shows the fusion of audio and video histogram of the surrounding environment of the robot to enable the sensory and perception communication of the robot.

A few findings from the tests, the efficiency of both systems is degraded amid the daylight when the luminance and shades of the objects are impacted by the light entering the room via the glass. Even though audio computation is speedier than visual handling, the percentage of recognition distances in the histogram bins is set to 18 in sequence to evaluate a considerable number of specimens for the histogram (in which the quantity of containers is the value that, when multiplied by itself gives the number of an amount of specimen), with the alternate amount as the prominent one.

The evaluation, multimodal sensor depiction is given using the red circle inside appropriate pictures for the bins inside the field of vision, marking the overall mean of the proto-object having greatest striking. The acquired findings is displayed under brightness circumstances: day and night. In all situations, the findings revealed that the multimodal sensor outperformed the OpenCV estimate.

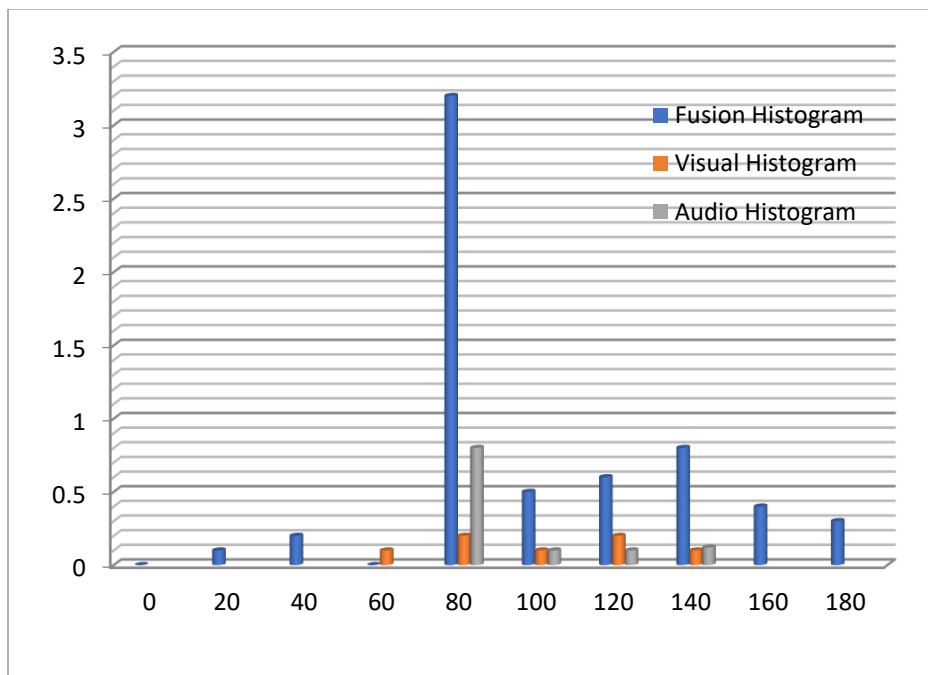


Figure 3: The sensory communication evaluation of the robot.

6. Conclusion

Focusing on a multimodal sensor this scientific paper provides a technique for identifying and following a speaker. The technique used to build this sensor comprises of integrating visual and auditory information regarding the existence of a presenter utilizing a Bayes model. The instinctive strategy is used in pair of methods. Foremost, for the specific instance of identifying a speaker located in the environment, the human learning procedure is modelled with a training procedure used to construct up a maximal posterior matrix wherein variables and observations are connected. Secondly, rather than utilizing more sophisticated and economically expensive techniques, the multimodal sensor is constructed by integrating information collected with two videocam era and the pair of mics, like people do (greater quantity of mic further available sensors, like that of deepness in camera and melting camera).

This proposed method may allow robots to monitor a human in everyday situations by using a bio-inspired technique with a minimal resource requirement. Furthermore, the system is prepared to add methods that will enable it to monitor many presenters by utilizing the evidence likelihood characterization provided by histograms. Moreover, as upcoming work, we are currently focusing on adding methods to recognize many presenters without having to specify the number of energetic sources ahead of time.

REFERENCE

1. Libin, A; Cohen-Mansfield, J. Therapeutic robot for nursing home residents with dementia: Preliminary inquiry. *Am. J. Alzheimers Dis. Other Demen.* 2004, 19, 111–116.
2. Fong, T.; Nourbakhsh, I.; Dautenhahn, K. A survey of socially interactive robots. *Robot. Auton. Syst.* 2003, 42, 143–166.
3. Koene, A.; Moren, J.; Trifa, V.; Cheng, G. Gaze shift reflex in a humanoid active vision system. In *Proceedings of the 5th International Conference on Computer Vision Systems, Bielefeld, Germany, 21–24 March 2007.*
4. Moren, J.; Ude, A.; Koene, A.; Cheng, G. Biologically based top-down attention modulation for humanoid interactions. *Int. J. Humanoid Robots* 2008, 5, 3–24.
5. Ferreira, J.F.; Lobo, J.; Bessiere, P.; Castelo-Branco, M.; Dias, J. A Bayesian Framework for Active Artificial Perception. *IEEE Trans. Cybern.* 2013, 43, 699–711.
6. Nakamura, K.; Nakadai, K.; Asano, F.; Ince, G. Intelligent sound source localization and its application to multimodal human tracking. In *Proceedings of the IEEE IROS, San Francisco, CA, USA, 25–30 September 2011; pp. 143–148.*
7. Rennie C, Shome R, Bekris KE, Souza AF. A dataset for improved RGBD-based object detection and pose estimation for warehouse pick-and-place. *IEEE Robotics and Automation Letters.* July 2016; 1(2), pp. 1179-1185.
8. Bore N, Jensfelt P, Folkesson J. Multiple object detection, tracking and long-term dynamics learning in large 3D maps. *CoRR*, <https://arxiv.org/abs/1801.09292>. 2018.
9. Handa A, Patraucean V, Badrinarayanan V, Stent S, Cipolla R. Understanding real world indoor scenes with synthetic data. 2016 IEEE Conference on Computer Vision and Pattern Recognition (CVPR), Las Vegas, NV, 2016, pp. 4077-4085.

10. Firman M. RGBD datasets: Past, present and future. Firman 2016 RGBDDP, In: 2016 IEEE Conference on Computer Vision and Pattern Recognition Workshops (CVPRW) on Large Scale 3D Data: Acquisition, Modelling and Analysis; 2016. 661-673.
11. Sünderhauf N, Dayoub F, McMahon S, Talbot B, Schulz R, Corke P, Wyeth G, Upcroft B, Milford M. Place categorization and semantic mapping on a mobile robot. In: IEEE International Conference on Robotics and Automation (ICRA); Stockholm; 2016. pp. 5729-5736.
12. Brucker M, Durner M, Ambrus R, Csaba Marton Z, Wendt A, Jensfelt P, Arras KO, Triebel R. Semantic labeling of indoor environments from 3D RGB maps. In: IEEE/RSJ International Conference on Intelligent Robots and Systems (IROS); 2018.
13. Saarinen J, Andreasson H, Lilienthal AJ. Independent Markov chain occupancy grid maps for representation of dynamic environment. In: IEEE/RSJ International Conference on Intelligent Robots and Systems (IROS); 2012. pp. 3489-3495.
14. Fong T, Nourbakhsh I, Dautenhahn K. A survey of socially interactive robots. *Robotics and Autonomous Systems*. 2003; 42(3-4):143-166.
15. Diego R. Faria, Mario Vieira, Premebida C, Nunes U. Probabilistic human daily activity recognition towards robot-assisted living. In: Proceedings of the IEEE RO-MAN'15; Japan; 2015.
16. Manduchi R, Castano A, Talukder A, Matthies L. Obstacle detection and terrain classification for autonomous off-road navigation. *Autonomous Robots*. 2005; 18(1):81-102.
17. Fernandes R, Premebida C, Peixoto P, Wolf D, Nunes U. Road detection using high resolution LIDAR. In: IEEE Vehicle Power and Propulsion Conference, IEEE-VPPC; 2014.
18. Asvadi A, Garrote L, Premebida C, Peixoto P, Nunes UJ. Multimodal vehicle detection: Fusing 3D LIDAR and color camera data. *Pattern Recognition Letters*. Elsevier. 2017.
19. Premebida C, Nunes U. Fusing LIDAR, camera and semantic information: A context-based approach for pedestrian detection. *The International Journal of Robotics Research*. 2013; 32(3):371-384.
20. Sünderhauf N, Brock O, Scheirer W, Hadsell R, Fox D, Leitner J, Upcroft B, Abbeel P, Burgard W, Milford M, Corke P. The limits and potentials of deep learning for robotics. *The International Journal of Robotics Research*. 2018;37(4-5):405-420.
21. Suresh, P., Ravikumar O, Hari Krishna Mahesh K, Sri Aashritha S, 2020 "Content Extraction Through Chatbots With Artificial Intelligence Techniques," *International Journal of Scientific & Technology Research*, Vol. 9, Issue 02, pp. 1960-1963.
22. Hornung A, Wurm KM, Bennewitz M, Stachniss C, Burgard W. OctoMap: An efficient probabilistic 3D mapping framework based on octrees. *Autonomous Robots*. 2013.
23. Suresh, P., Saravanakumar, U., Celestine Iwendji, Senthilkumar Mohan, Gautam Srivastav 2020 "Field-programmable gate arrays with low power vision system using dynamic switching" *Computers & Electrical Engineering*, Vol. 90, 2021, 106996.
24. Cadena C, Carlone L, Carrillo H, Latif Y, Scaramuzza D, Neira J, Reid I, Leonard JJ. Past, present, and future of simultaneous localization and mapping: Toward the robust-perception age. *IEEE Transactions on Robotics*. 2016; 32(6):1309-1332.
25. Biber P, Duetz T. Experimental analysis of sample-based maps for long-term SLAM. *The International Journal of Robotics Research*. 2009;28:20-33.

26. Walcott-Bryant A, Kaess M, Johannsson H, Leonard JJ. Dynamic pose graph SLAM: Long-term mapping in low dynamic environments. In: IEEE/RSJ International Conference on Intelligent Robots and Systems (IROS); 2012. pp. 1871-1878.
27. Andreasson H, Magnusson M, Lilienthal A. Has something changed here? Autonomous difference detection for security patrol robots. In: IEEE/RSJ International Conference on Intelligent Robots and Systems (IROS); 2007. pp. 3429-3435.
28. Hermans A, Floros G, Leibe B. Dense 3D semantic mapping of indoor scenes from RGB-D images. In: IEEE International Conference on Robotics and Automation (ICRA), Hong Kong; 2014. pp. 2631-2638.
29. Krahenbuhl P, Koltun V. Efficient inference in fully connected CRFs with Gaussian edge potentials. *Advances in Neural Information Processing Systems*. 2016; 24:109-117.
30. McCormac J, Handa A, Davison A, Leutenegger S. SemanticFusion: Dense 3D semantic mapping with convolutional neural networks. In: IEEE International Conference on Robotics and Automation (ICRA), Singapore; 2017. pp. 4628-4635.
31. Suresh. P., "Creation of optical chain in the focal region of high NA lens of tightly focused higher order Gaussian beam", Springer – Journal of Optics, Vol. 46, p. 225 – 230, 2017.
32. Ambrus R, Claiç S, Wendt A. Automatic room segmentation from unstructured 3-D data of indoor environments. *IEEE Robotics and Automation Letters*. 2017; 2(2):749-756.
33. Ambrus R, Bore N, Folkesson J, Jensfelt P. Autonomous meshing, texturing and recognition of object models with a mobile robot. In: IEEE/RSJ International Conference on Intelligent Robots and Systems (IROS), Vancouver, BC. 2017. pp. 5071-5078.
34. Armeni I, Sener O, Zamir AR, Jiang H, Brilakis I, Fischer M, Savarese S. 3D semantic parsing of large-scale indoor spaces. In: IEEE Conference on Computer Vision and Pattern Recognition (CVPR), Las Vegas, NV; 2016. pp. 1534-1543.
35. Suresh P., Aanandha Saravanan K., Celestine Iwendi, Ebuka Ibeke, Gautam Srivastava, "An artificial intelligence based quorum system for the improvement of the lifespan of sensor networks," *IEEE sensors journal*, Vol. 21, Issue: 15, pp. 17373 – 17385, 2021.
36. Nakadai, K.; Hidai, K; Mizoguchi, H.; Okuno, H.G.; Kitano, H. Real-Time Auditory and Visual Multiple-Object Tracking for Humanoids. In *Proceedings of the 17th International Joint Conference on Artificial Intelligence (IJCAI01)*, Seattle, WA, USA, 4–10 August 2011; Volume 2, pp. 1425–1432.
37. Asano, F.; Yamamoto, K.; Hara, I.; Ogata, J.; Yoshimura, T.; Motomura, Y.; Ichimura, N.; Asoh, H. Detection and Separation of Speech Event Using Audio and Video Information Fusion and Its Application to Robust Speech Interface. *EURASIP J. Adv. Sig. Proc.* 2004, 2004, 1727–1738.
38. Hara, I.; Asano, F.; Asoh, H.; Ogata, J.; Ichimura, N.; Kawai, Y.; Kanehiro, F.; Hirukawa, H.; Yamamoto, K. Robust speech interface based on audio and video information fusion for humanoid HRP-2. *Proc. IROS 2004*, 3, 2404–2410.